Detecting Rat Heart Myocardial Fiber Directions in X-ray Microtomography Using Coherence-Enhancing Diffusion Filtering

Birgit Stender and Alexander Schlaefer

Medical Robotics, Institute for Robotics and Cognitive Systems, University of Lübeck, Germany
{stender,schlaefer}@rob.uni-luebeck.de
http://www.rob.uni-luebeck.de/

Abstract. Because the electrical and mechanical properties of myocardial tissue are strongly anisotropic the local fiber direction is an important parameter for realistic computational models of cardiac excitation and motion. Within the last years Diffusion Tensor Imaging has been established as a noninvasive measuring technique for fiber directions from whole hearts ex vivo. X-ray microtomography offers a much higher spatial resolution than Diffusion Tensor Imaging and could scan a whole heart as well. The inherently low soft-tissue contrast can be enhanced through staining with iodine. We recorded a volumetric scan of a rat heart and filtered the imaging data with a coherence-enhancing anisotropic diffusion filter to enhance its microstructure. The filtering was performed in three dimensions. From the structure tensor of the filtered volumes scalar measurements and fiber tracts were calculated and used for visualization and further analysis.

1 Introduction

Information about the three-dimensional fiber direction in myocardial tissue is a key determinant for realistic simulations on excitation propagation in myocardial tissue. Electrical and mechanical properties important for the propagation of the depolarization front and the evoked contraction are strongly anisotropic, [13,6]. The microstructure of the heart is known to be changed by cardiac diseases like myocardial infarction (MI) or ventricular hypertrophy, [12]. A detailed knowledge of these so-called remodeling processes would help to improve computational models of diseased hearts and to quantify the effects of potential cures like the injection of stem cells on the remodeled myocardium.

Remodeling processes in the atria are also known as potential cause and consequence of atrial fibrillation, [8,1]. One option for the treatment of paroxysmal and persistent atrial fibrillation is pulmonary vein isolation (PVI) achieved by ablation. The process of scar building after ablation is not fully understood. A detailed analysis of fiber structure might explain the recurrence of arrhythmia in some patients after initial treatment success and could help to optimize ablation parameters.

So far different imaging modalities have been used for the detection of ex vivo fiber directions including confocal microscopy, Diffusion Tensor Imaging (DTI) and recently ultrasound and Optical Coherence Tomography (OCT) [4,9,2]. Among these imaging modalities DTI is the only option for the examination of a heart in whole. DTI provides

S. Ourselin, D. Rueckert, and N. Smith (Eds.): FIMH 2013, LNCS 7945, pp. 63–70, 2013.

insight into the diffusion tensor of water in tissue and is validated against histological findings, [5]. Still the measurement values are rather macroscopic because the resolution is in the range of millimeters even for modern MRI scanners. In case of strong interfacial differences in magnetic susceptibility imaging artifacts occur. Due to these characteristics the use of DTI is limited for hearts smaller in size than a canine heart and myocardial structures thinner in wall thickness than the ventricles.

The only imaging modality capable to scan the whole volume of a heart on the one hand and offering a resolution in the range of the diameter of a myocardial fiber is X-ray microtomography (micro-CT). Recently it has been shown that micro-CT can be used to segment the cardiac conduction system (CCS) of mammalian hearts, [11]. We adopted the staining technique described in this work for the imaging of rat hearts after optical mapping experiments to recover myocardial fiber directions from the volumetric scans.

2 Material and Methods

In diffusion-weighted imaging (DWI), different directions of the magnetic field gradient are applied to measure the rate of water diffusion in tissue. Based on the different excitations a symmetric positive definite diffusion tensor $\mathbf{D}$ is estimated with the following eigenvalue decomposition:

$$\mathbf{D} = \begin{pmatrix} v_{d,1} & v_{d,2} & v_{d,3} \end{pmatrix} \cdot \begin{pmatrix} \lambda_{d,1} & 0 & 0 \\ 0 & \lambda_{d,2} & 0 \\ 0 & 0 & \lambda_{d,3} \end{pmatrix} \cdot \begin{pmatrix} v_{d,1}^T \\ v_{d,2}^T \\ v_{d,3}^T \end{pmatrix} . \tag{1}$$

As illustrated in Fig. 1 b) The first eigenvector $v_{d,1}$ gives the local direction of the myocardial muscle fiber. The second eigenvector $v_{d,2}$ is orthogonal to $v_{d,1}$ and parallel to the fiber sheet. The third eigenvector $v_{d,3}$ is the cross product of the first two. The ratios between the eigenvalues of the diffusion tensor are a measure for the anisotropy with respect to water diffusion.

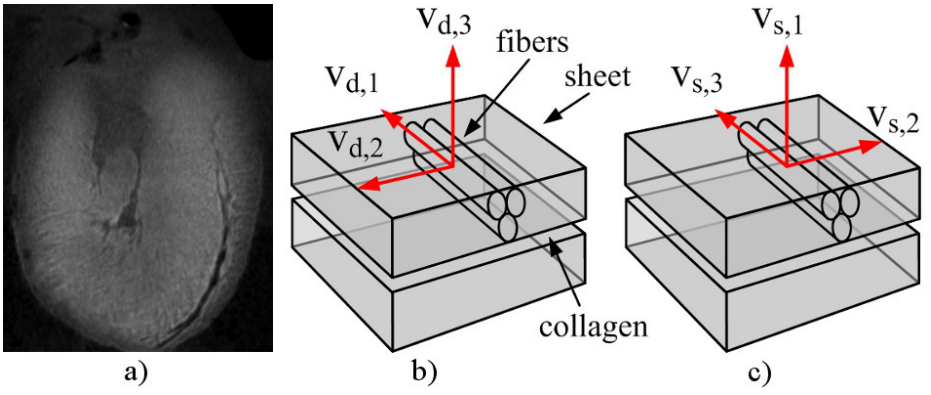

Fig. 1. (a) Micro-CT volumetric scan of the rat heart in long-axis view. Eigenvector orientation of the diffusion tensor (b) and structure tensor (c) with respect to the myocardial microstructure.

For a structure in an image volume a very similar measure can be determined from the image intensity values, the structure tensor $\mathbf{J}$. It is a measure of the structural anisotropy. The first eigenvector $v_{s,1}$ is aligned with the average local orientation of the gradient, the third eigenvector $v_{s,3}$ is the average direction of the most homogeneous structure.

The approach we used to evaluate this tensor was divided in the following steps:

- A micro-CT volume of a whole rat heart was filtered using anisotropic diffusion filtering to enhance the microstructure.
- From the filtered micro-CT volumes the structure tensor distribution was determined.
- The structure tensors were transformed into a diffusion tensors.
- The diffusion tensor field was then used to calculate scalar measures and fiber tracts.

2.1 Material

The rat heart examined was taken from an animal subject of a series of neurological experiments. The animals in this series were deeply anesthetized with isopropanol and decapitated. The heart was dissected and given into oxygenated ice-cold modified Tyrode solution. The heart was prepared as pressure-controlled isolated beating heart and optical experiments were performed. After finishing these experiments a Tyrode solution with 5% iodine was injected via the aortic canula into the coronary arteries. The heart was placed inside this solution for 24 hours and frozen in 0.9% salt solution afterwards. A volumetric micro-CT scan with 17.4 μm spatial resolution was recorded while the heart was placed on an actively cooled probe holder. The image volume without filtering is displayed in Fig. 1 a).

2.2 Coherence-Enhancing Anisotropic Diffusion Filtering

The myocardial fiber direction is only slightly visible within computed tomography images because of the limited contrast of soft tissue in x-ray. Conventional edge detection algorithms fail in detecting the fiber direction because the microstructure does not consist of straight lines neither in a Cartesian nor in a prolate coordinate system. In short axis view the imaging structure is forming a curl. Diffusion filtering is an approach initially presented by Weickert, [14]. It has been successfully applied on similar problems like filtering fingerprints to achieve continuous edges, [3]. The main idea of anisotropic diffusion filtering is to mimic a diffusion process

$$\frac{\partial u}{\partial t} = -\nabla \cdot j \tag{2}$$

which bias the flux j towards interesting imaging features in the distribution of gray values u in the image. Creating such a flux requires the introduction of an anisotropic diffusion tensor $\mathbf{D}$:

$$\frac{\partial u}{\partial t} = -\nabla \cdot (\mathbf{D} \cdot \nabla u) \tag{3}$$

The diffusion tensor is calculated from the structure tensor

$$\mathbf{J} = h_\rho * \nabla u_\sigma \nabla u_\sigma^T, \tag{4}$$

where ∇u_σ is the prefiltered gradient of the imaging gray values. h_ρ denotes a Gaussian blurring kernel with standard deviation ρ. The parameter σ is the standard deviation of the Gaussian kernel used for the prefiltering.

While the application of a linear diffusion process is equivalent to the convolution with a Gaussian kernel having a time-dependent standard deviation, the kernel function in anisotropic diffusion filtering is a Gaussian kernel ellipsoidal deformed by the diffusion tensor. In imaging regions with uniform gray value distribution the filtering effect is the same as for the linear diffusion process. In presence of edges the major axis of the ellipsoidal Gaussian kernel are aligned with the curvature. To enhance flow-like structures, the diffusion tensor eigenvalues suggested in [14] for coherence-enhancing filtering were applied.

2.3 Relevant Parameters and Schemes for Calculating the Spatial Derivatives

Because equation (3) can not be solved analytically its solution needs to be determined by means of numerical integration. We used a simple forward euler scheme. To assure stability a discretization of $dT = 1$ was found to be sufficiently small. The filtering results depend on three parameters and the choice of the numerical scheme for calculating the spatial derivatives. These parameters are first, σ, the standard deviations of

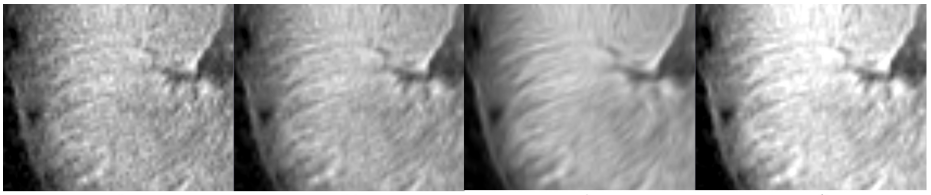

Fig. 2. Effect of different schemes for the evaluation of the divergence operator equation. (a) Original image section within a long-axis plane, (b) filtered using the standard scheme, (c) the rotational invariant scheme and (d) the optimized rotational invariant scheme. Parameters: $\sigma = 1$, $\rho = 10$ and $T = 10$.

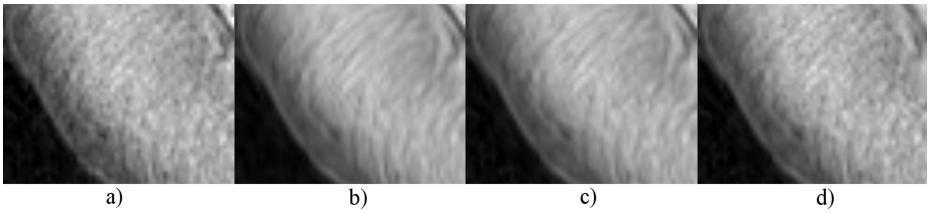

Fig. 3. Evaluation of the prefilter standard deviation σ. The original image is displayed in a). The parameter was set to $\sigma = 1$ (b), $\sigma = 3$ (c) and $\sigma = 10$ (d).

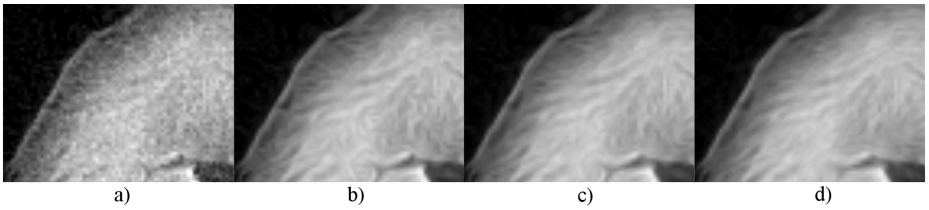

Fig. 4. Effect of the regularization parameter ρ. The original image is displayed in a). The parameter was set to $\rho = 5$ (b), $\rho = 10$ (c) and $\rho = 25$ (d).

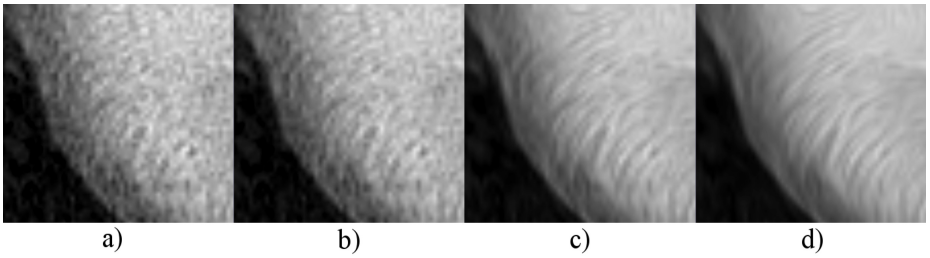

Fig. 5. Influence of the integration time T. The original image is displayed in a). Integration time was set $T = 1$ (b), $T = 10$ (c) and $T = 25$ (d).

the Gaussian filter applied before spatial derivates were determined. Second, the standard deviation ρ of the regularizing filter applied on the structure tensor according to eqn:structTensor. Third, the integration time T for the diffusion process in equation (3). Different schemes for calculating the spatial derivatives of the right-hand side of the diffusion equation were compared. The standard scheme uses central differences with previously applied Gaussian filtering. A more rotational invariant scheme is achieved using a Sobel filter with values of Scharr, [15]. A third scheme presented in [7], which includes kernel parameters optimized for rotational invariance, was tested.

The best choice of parameters was systematically explored by means of visual inspection and in exchange with biomedical experts working with confocal microscopy on structural analysis of rat hearts.

2.4 Fiber Tractography

Due to the clinical relevance of fiber tracking in DTI volumes fiber tractography is already a well established technique [16]. Different approaches are already integrated as modules in tools for medical image analysis and operation planning. We used 3D Slicer for fiber tracking and diffusion visualization [10]. A label map was assigned within a few short-axis slices to generate seed points for the tracking algorithm. A threshold on the fractional anisotropy was defined as stopping criterion.

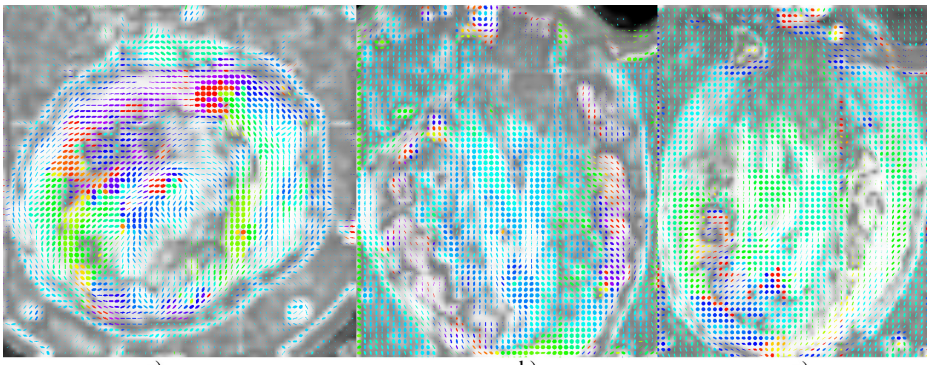

a) b) c)

Fig. 6. Ellipsoidal Glyphs of the diffusion tensor displayed on the scalar volume of the diffusion tensor trace distribution. The ellipsoids are colored according to their orientation. The three orthogonal planes displayed are the short-axis xy-plane (a), long-axis xz-plane (b) and long-axis yz-plane (c).

3 Results

3.1 Comparing the Effect of Different Schemes

In Fig. 2 the filtering effect of the three different schemes is displayed for comparison. For the standard scheme used for the result displayed in 2 b) an inhomogeneous filtering effect can be observed. Lines which run parallel to the axes of the Cartesian coordinate system are more enhanced than edges with other directions. Between the rotational invariant schemes in c) and d) the only difference seems to be a slightly increased contrast of the optimized scheme in Fig. 2 d). We decided to use the simpler rotational invariant scheme corresponding to the result in Fig. 2 c).

3.2 Evaluation of Parameter Sensitivity

We have found the microstructure enhancing to be sensitive towards an increase of σ to values larger than 1 as displayed in Fig. 3. This behavior might be caused by a spatial resolution in the range of a fiber diameter. In Fig. 5 the effect of the integration time is displayed for $T = 1, 10, 25$ from left to right. Based on visual inspection we decided to use $T = 10$ for the integration time and $\rho = 15$ for the standard deviation of a Gaussian filter applied afterwards to achieve a good compromise between structure enhancement and over-regularization. For the filtering results shown in Fig. 3 to Fig. 5 only one parameter at a time changed, the other two are remain optimal.

3.3 Fiber Orientation

From the filtered mico-CT volumes the distribution of the diffusion tensor $\mathbf{D}$ was calculated with the same parameter values $\sigma = 1$ and $\rho = 10$ as previously applied for the

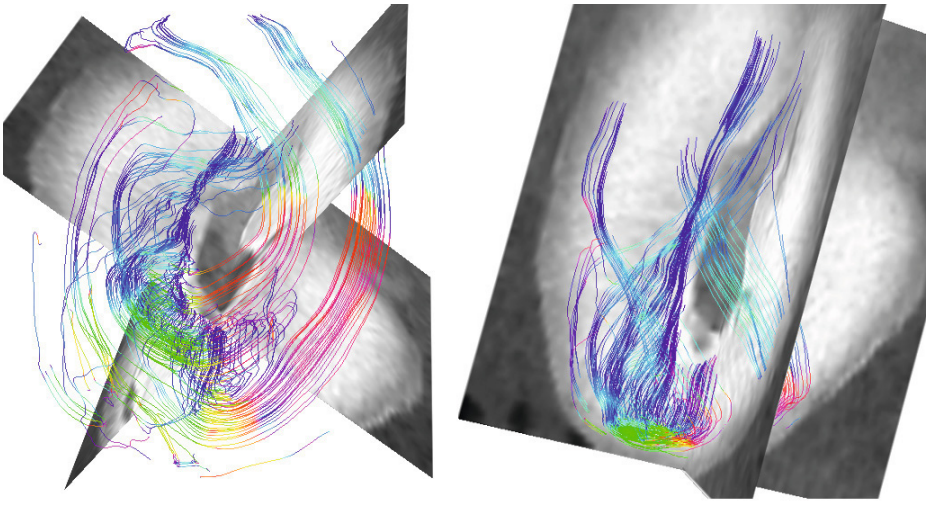

Fig. 7. Fiber tracts generated from a region of interest defined at the apex. a) Looking at the apex b) Looking at the left ventricle.

structure-enhancing filtering. From the diffusion tensor field scalar measures like fractional anisotropy or the trace can be determined. In Fig. 6 three orthogonal projections of the trace field are displayed with an overlay of ellipsoidal glyphs. The main axes of the ellipsoids are aligned with the diffusion tensor eigenvectors. Their orientation is shown color-coded.

The finally determined three-dimensional fiber tracts along with orthogonal projections of the filtered micro-CT volume are displayed in Fig. 7. On the left hand-side a view from the apex of the heart reveals a curled fiber direction in left ventricular myocardium. On the right hand-side fibers are visible following a structure which might is a part of the Purkinje-Fiber network.

4 Conclusion

To our knowledge we have introduced for the first time an approach for three-dimensional myocardial fiber detection from micro-CT volumetric scans. We were able to detect epicardial fiber directions in accordance with the directions reported in the literature. By calculating the But so far the described twist of the myocardial fiber direction along transmural axis in the left ventricle could not be observed. Because histological findings are regarded as gold standard for the detection of fiber direction we will further histologically examine the scanned heart to validate our results.

References

1. Allessie, M., Ausma, J., Schotten, U.: Electrical, contractile and structural remodeling during atrial fibrillation. Cardiovasc. Res. 54(2), 230–246 (2002)
2. Goergen, C.J., Radhakrishnan, H., Sakadic, S., Mandeville, E.T., Lo, E.H., Sosnovik, D.E., Srinivasan, V.J.: Optical coherence tractography using intrinsic contrast. Opt. Lett. 37(18), 3882–3884 (2012)
3. Gottschlich, C., Schönlieb, C.-B.: Oriented diffusion filtering for enhancing low-quality fingerprint images. IET Biometrics 1(2), 105–113 (2012)
4. Helm, P., Beg, M.F., Miller, M.I., Winslow, R.L.: Measuring and mapping cardiac fiber and laminar architecture using diffusion tensor MR imaging. Ann. N. Y. Acad. Sci. 1047, 296–307 (2005)
5. Holmes, A.A., Scollan, D.F., Winslow, R.L.: Direct histological validation of diffusion tensor MRI in formaldehyde-fixed myocardium. Magn. Reson. Med. 44(1), 157–161 (2005)
6. Klber, A.G., Rudy, Y.: Basic mechanisms of cardiac impulse propagation and associated arrhythmias. Physiol. Rev. 84(2), 431–488 (2004)
7. Kroon, D.-J., Slump, C.H., Maal, T.J.J.: Optimized anisotropic rotational invariant diffusion scheme on cone-beam CT. In: Jiang, T., Navab, N., Pluim, J.P.W., Viergever, M.A. (eds.) MICCAI 2010, Part III. LNCS, vol. 6363, pp. 221–228. Springer, Heidelberg (2010)
8. Kumar, S., Teh, A.W., Medi, C., Kistler, P.M., Morton, J.B., Kalman, J.M.: Atrial remodeling in varying clinical substrates within beating human hearts: relevance to atrial fibrillation. Prog. Biophys. Mol. Biol. 110(2-3), 278–294 (2012)
9. Lee, W.N., Larrat, B., Pernot, M., Tanter, M.: Ultrasound elastic tensor imaging: comparison with MR diffusion tensor imaging in the myocardium. Phys. Med. Biol. 57(16), 5075–5095 (2012)
10. Pieper, S., Halle, M., Kikinis, R.: 3D slicer. In: Proceedings of the 1st IEEE International Symposium on Biomedical Imaging: From Nano to Macro, pp. 632–635 (2004)
11. Stephenson, R.S., Boyett, M.R., Hart, G., Nikolaidou, T., Cai, X., Corno, A.F., Alphonso, N., Jeffery, N., Jarvis, J.C.: Contrast enhanced micro-computed tomography resolves the 3-dimensional morphology of the cardiac conduction system in mammalian hearts. PLoS One 7(4), e35299 (2012)
12. Sun, Y.: Myocardial repair/remodelling following infarction: roles of local factors. Cardiovasc. Res. 81(3), 482–490 (2009)
13. Valderrbano, M.: Influence of anisotropic conduction properties in the propagation of the cardiac action potential. Prog. Biophys. Mol. Biol. 94(1-2), 144–168 (2007)
14. Weickert, J.: Anisotropic Diffusion in Image Processing. Teubner-Verlag, Stuttgart (1998)
15. Weickert, J., Scharr, H.: A scheme for coherence-enhancing diffusion filtering with optimized rotation invariance. J. Vis. Commun. Image Represent. 13(1), 103–118 (2002)
16. Zhukov, L., Barr, A.H.: Heart-muscle fiber reconstruction from diffusion tensor MRI. In: Proceedings of the 14th IEEE Visualization 2003 (VIS 2003), vol. 79, IEEE Computer Society (2003)